Towards an unified description of total and diffractive structure functions at HERA in the QCD dipole picture

A. Bialas,*RP eschanski†and Ch. Royon‡

December 3, 1997

Abstract

It is argued that the QCD dipole picture allows to build an unified theoretical description -based on BFKL dynamics- of the total and diffractiven ucleon structure functions. This description is in qualitative agreement with the present collection of data obtained by the H1 collaboration. More precise theoretical estimates, in particular the determination of the normalizations and proton transverse momentum behaviour of the diffractive components, are shown to be required in order to reach definite conclusions.

1 Motivation

Considering the phenomenological discussion on the proton structure functions measured by deep-inelastic scattering of electrons and positrons at HERA, it is striking to realize that the proposed models, on one side for

---

*Institute of Physics, Jagellonian University, Reymonta 4, 30-059 Cracow, Poland

†CEA, Service de Physique Théorique, CE-Saclay, F-91191 Gif-sur-Yvette Cedex, France

‡CEA, DAPNIA, Service de Physique des Particules, CE-Saclay, F-91191 Gif-sur-Yvette, France

1

the total quark structure function $F_2(x, Q^2)$ [1] and on the other side for its diffractive component $F_2^{D(3)}(x, M^2, Q^2)$ [2] are in general distinct. Indeed, the models [3] aiming at the description of $F_2(x, Q^2)$ use a QCD-inspired "hard Pomeron" parametrisation related either to a DGLAP [4] evolution with extrapolation at small-x [5] or to BFKL [6] dynamics. On the other hand, most of the models proposed for the diffractive component of the quark structure function rely on a "soft Pomeron" picture of diffraction, assuming a point-like structure of the Pomeron considered as a compound particle [7].

It is known since some time, however, that at high energies the elastic scattering and diffraction dissociation of hadrons are closely related [8], being both a reflection of the same phenomenon, namely *absorption* of the incident particle wave in the target. It seems therefore interesting to verify if the same applies also to the incident virtual photons.

In the present paper we investigate this question in the framework of the QCD dipole picture [10, 11]. This picture turned out already to be successful in the description of the total virtual photon-nucleon cross-section (i.e. of total nucleon structure function F_2 [12]). The purpose of the present paper is to verify if the so-called rapidity gap events [3] discovered recently at HERA can also be described along these lines. Diffractive dissociation of the virtual photons in the framework of the QCD dipole picture was recently discussed in [13, 14]. It was argued that the diffractive cross-section consists of two components:

-(component I) the *inelastic* component when the gluon cascade which evolved from the incident virtual photon interacts inelastically with the target, see Fig.1a. This component (corresponding to the 3-Pomeron interaction in the Regge terminology) contributes mainly to the region of very large mass M of the diffractively excited system: $\beta << 1$, where, as usual, $\beta = Q^2/(Q^2 + M^2)$.

-(component II) the *quasi-elastic* component when the $q\bar{q}$ pair emerging from the virtual photon scatters elastically from the target, see Fig.1b. This component contributes to the region of smaller masses $\beta \geq .2$.

The model calculations of Refs. [13, 14] provided the formulae for differential cross-section $d\sigma/dM^2$ of both components I and II. Unfortunately, for technical reasons, some rather drastic assumptions had to be made:

(a) The calculations were performed in the limit of large impact parameters. The integrated cross-section was then estimated by integration only up

2

to a certain cut-off b_{min}. This procedure leads to a serious underestimate of the cross-section [17].

(b) The target nucleon was treated as a collection of several QCD dipoles all of the same size and sitting at one point. This assumption neglects the effects of nucleon form-factor and thus leads to an overestimation of the cross-sections.

We are thus led to the conclusion that there are at present no reliable predictions for the *absolute normalization* of the diffractive cross-sections of the virtual photons. In this situation, in order to compare the predictions with the data we decided to treat the normalization constants in the two components as arbitrary parameters and restrict ourselves to the comparison of the observed dependence on kinematic variables to that predicted by the formulae of Refs. [13, 14] (c.f. also [15]). Our work should thus be treated as an exploratory search which is a guide for further investigation and should be repeated once more reliable calculations are available. Within these *caveats* our investigation leads to the conclusion that the data on rapidity gap events published recently by H1 collaboration [2] are reasonably well described by the QCD dipole picture and thus the Good-Walker idea seems consistent with these data.

The plan of our investigations is as follows. In the next section we remind briefly the QCD dipole picture results for the total photon-nucleon cross-section, introduce the necessary notation and perform a fit for the total structure function. In Section 3 we summarize the formulae for diffractive cross-section of the components (I) and (II). These results are compared to the data [2] in Section 4. Finally Section 5 contains our conclusions, as well as an outlook for further work.

2   Proton structure functions

In the QCD-dipole picture of high-energy scattering of two initial small-size $(r, \bar{r})$ *onia* (massive $q\bar{q}$ states), the total cross-section at fixed impact parameter $\sigma(b)$ can be obtained from the all-order QCD resummation of the elementary dipole-dipole cross-sections $\sigma(\rho, \bar{\rho})$ where dipole states of transverse diameter ρ (resp. $\bar{\rho}$) appear in the wave-function of the initial states of transverse diameter r (resp. $\bar{r}$) at the "time" of interaction. This "time" variable is represented by a rapidity variable $\ln c/\xi$, where c is a phenomeno-

3

logical constant [16] and ξ is the Bjorken variable labelling the softer end of the produced dipole . One writes

$$\sigma_{tot} = \int d^2b \; \sigma(b) = \int \frac{d\rho}{\rho} n_1\left(r; \rho, \xi\right) \int \frac{d\bar{\rho}}{\bar{\rho}} n_1\left(\bar{r}, \bar{\rho}, \bar{\xi}\right) \; \sigma\left(\rho, \bar{\rho}\right), \tag{1}$$

where the partition of the total "time" $\ln c/x = \ln c/\xi\bar{\xi}$ between the target and projectile is arbitrary, provided $\xi\bar{\xi} = x$. $n_1\left(r, \rho, \xi\right)$ is the multiplicity of dipoles of size ρ, integrated over the transverse distance from the center of the onium, generated from an initial dipole of size r after a "time" $\ln c/\xi$. It is given by

$$n_1(r, \rho, \xi) = \int \frac{d\gamma}{2\pi i} \; \left(\frac{r}{\rho}\right)^{\gamma} \; e^{\Delta(\gamma)\ln(1/\xi)} \tag{2}$$

where

$$\Delta(\gamma) = \frac{\alpha N}{\pi}\left(2\psi(1) - \psi(1 - \gamma/2) - \psi(\gamma/2)\right) \tag{3}$$

is the eigenvalue of the BFKL kernel [6], and $N = 3$ is the number of colours.

The elementary dipole-dipole cross-sections are obtained from the gluon-exchange graphs and give [10]

$$\sigma\left(\rho, \bar{\rho}\right) = 8\pi\alpha^2 \int \frac{d\ell}{\ell^3} \left[1 - J_0\left(\ell\rho\right)\right]\left[1 - J_0\left(\ell\bar{\rho}\right)\right] i$$

$$= 2\pi\alpha^2 \rho_<^2 \left[1 + \ln(\rho_>/\rho_<)\right]. \tag{4}$$

Inserting formulae (2) and (4) in the cross-section formula (1), one finds

$$\sigma(r, \bar{r}, \xi) = 2\pi\alpha^2 r\bar{r} \int \frac{d\gamma}{2\pi i} \left(\frac{r}{\bar{r}}\right)^{\gamma-1} \frac{4}{\gamma^2(2 - \gamma)^2} \; e^{\Delta(\gamma)\ln(1/\xi)} \tag{5}$$

In order to obtain the virtual photon-proton cross-section from (5) one has to integrate over the initial distributions of dipoles inside the photon and the proton. Since we know neither the number nor the distribution of the dipoles in the proton, we simply define

$$\int d^2\bar{r} \; (\bar{r})^{2-\gamma} \; \Phi(\bar{r}) \equiv \; n_{eff}(\gamma) \; [r_0(\gamma)]^{2-\gamma} \tag{6}$$

where n_{eff} has the meaning of the average number of primary dipoles in the proton and r_0 is their average transverse diameter.

4

The distributions of the primary dipoles in the virtual photons are known [18, 11] and thus the corresponding integrals can be performed with the result

$$\sigma_{T,L}(x, Q^2) = \frac{4N\alpha_{em}e_f^2}{\pi}\alpha^2 n_{eff} \int \frac{d\gamma}{2\pi i} r_0^2 \left(\frac{2}{Qr_0}\right)^\gamma e^{\Delta(\gamma)\ln(1/x)}$$

$$\times \frac{4}{\gamma^2(2-\gamma)^2} \frac{\Gamma^2(2-\gamma/2)\Gamma^4(1+\gamma/2)}{\Gamma(4-\gamma)\Gamma(2+\gamma)} H_{T,L}(\gamma) \qquad (7)$$

where

$$H_T(\gamma) = \frac{(2-\gamma/2)(1+\gamma/2)}{\gamma(1-\gamma/2)}, \quad H_L(\gamma) = 1. \qquad (8)$$

$H_{T,L}$ refers to transverse and longitudinal photons, respectively. e_f^2 is the total charge of the quarks whose flavour contributes to the reaction, and $n_{eff} = n_{eff}(1)$, $r_0 = r_0(1)$, see formula (6).

The path integral in (7) can be evaluated by the saddle point method (giving good approximation as $x \to 0$). The result is

$$F_{T,L} = \frac{Q^2}{4\pi^2\alpha_{em}}\sigma_{T,L} = H_{T,L}(1) \frac{\pi N\alpha^2 e_f^2}{32} n_{eff} \left(\frac{x}{c}\right)^{-\Delta_P} \frac{r_0 Q}{2}$$

$$\times \left(\frac{2a(x)}{\pi}\right)^{1/2} \exp\left\{-\frac{a(x)}{2}\ln^2\left(\frac{r_0 Q}{2}\right)\right\}. \qquad (9)$$

where $H_L(1) = 1$, $H_T(1) = 9/2$ and

$$a(\xi) = [7\alpha N\zeta(3)\ln(c/\xi)/\pi]^{-1}, \quad \Delta_P \equiv \Delta(1) = 4\ln 2 \, \alpha N/\pi \qquad (10)$$

are the well-known coefficients appearing in the solution of BFKL dynamics for the Pomeron [6].

Formula (9) gives the prediction for the nucleon structure functions in terms of four parameters: the strong coupling constant α, the average number of primary dipoles in the proton n_{eff}, their average radius r_0, and the constant c fixing the rapidity scale of the problem. It coincides with the one used in the published fit [12] apart the new parameter c which sets the rapidity scale of the process, and is unavoidable in the leading log approximation of QCD. This justifies a new fit of F_2 using formula (9) which we have performed assuming $\Delta_P = .282$ (as in [12]) and leaving free the three other parameters. The result is

$$\Delta_P = .282, \quad c = 1.75, \quad Q_0 = \frac{2}{r_0} = .622\text{GeV}, \quad n_{eff} = 3.8/e_f^2. \qquad (11)$$

5

The fit (displayed in Fig.2) is using the published data from the H1 experiment [1] . We have only considered the points with $Q^2 \leq 150\text{GeV}^2$ to remain in a reasonable domain of validity of the QCD dipole model. Changing this value does not appreciably change the quality and parameters of the fit. The χ^2 is 88.7 for 130 points. Although not included in the fit, the data points at high $Q^2 > 150\text{GeV}^2$ and $x < 5.10^{-1}$ are well described, while at higher x, an expected contribution of valence quarks is needed.

Commenting on the parameters, let us note that the effective coupling constant extracted from Δ_P is $\alpha = 0.11$, close to $\alpha(M_Z)$ used in the H1 QCD fit. It is an acceptable value for the small coupling constant required by the BFKL framework[1]. The value of Q_0 corresponds to a transverse radius of $0.4fm$ which is in the correct range for a proton non-perturbative characteristic scale. The value of n_{eff} determines the number of primordial dipoles in the proton to be about 6 (if three flavours contribute to the process) which also does not seem unreasonable. The parameter c sets the "time" scale for the formation of the interacting dipoles. It defines the effective total rapidity interval which is $\ln(1/x) + \ln c$, the constant being not predictable (but of order 1) at the leading logarithmic approximation.

The obtained fit for F_2 is very similar than the previously published one in Ref. [12], even with a better χ^2. In the same spirit, relation (11) provides a parameter-free prediction for the gluon density (not shown in the figures) which is, as the previous one [12], in good agreement with the results obtained by the H1 QCD fits based on a NLO DGLAP evolution equation [1]. Using the factorization properties of formula (11) and noting [12] that the F_L structure function is given by a similar formula with $h_T + h_L$ replaced by h_L, one obtains a parameter-free prediction for F_L (see Fig.3). Note that we obtain a prediction in agreement with the (indirect) experimental determination for F_L [20], but somewhat lower than the center values. Thus, it would be interesting to obtain a more precise measurement of F_L to test the different predictions on the Q^2-evolution as already mentionned in Ref. [12].

---

[1]The running of the coupling constant and other next leading log corrections are not taken into account in the present BFKL scheme. This could explain the rather low value of the effective Δ_P which is expected to be decreased by the next leading contributions [19].

3   Diffractive structure functions

The diffractive structure functions are related to the corresponding diffractive γ^*-nucleon cross-sections by the relation

$$F_{T,L}^{D(3)}\left(Q^2, x_P, \beta\right) \equiv \frac{Q^2}{4\pi^2\alpha_{\text{e.m.}}} x_P^{-1} \int d^2b \, \frac{\beta \, d\sigma_{T,L}}{d\beta \, d^2b}, \tag{12}$$

where $x_P = x/\beta$.

As already explained in the first section, in the QCD dipole model the diffractive structure functions are given by two components: inelastic and quasi-elastic. They were discussed in [13, 14] where the formulae for γ^*-dipole diffractive cross-sections were derived and used to construct the corresponding structure functions following the formula. These results are summarized below.

(I) Inelastic component.

$$F_{T,L}^{D(3),inel}(Q^2, x_P, \beta) = \frac{16e_f^2\alpha^5 N}{\pi} n_{eff}^2 \left(\frac{2a(x_P)}{\pi}\right)^3 x_P^{-1-2\Delta_P}$$

$$\int_{c-i\infty}^{c+i\infty} \frac{d\gamma}{2\pi i} \left(\frac{r_0 Q}{2}\right)^\gamma \Omega(\gamma) H_{T,L}(\gamma)\beta^{-\Delta(\gamma)} \tag{13}$$

where $H_{T,L}$ are defined in (8),

$$\Omega(\gamma) = V(\gamma)\frac{2}{\gamma(2-\gamma)^3}\frac{\Gamma^4(2-\gamma/2)\Gamma^2(1+\gamma/2)}{\Gamma(4-\gamma)\Gamma(2+\gamma)} \tag{14}$$

and

$$V(\gamma) = \int_0^1 {}_2F_1\left(1-\gamma, 1-\gamma; 1; y^2\right) dy \; . \tag{15}$$

($_2F_1$ is the hypergeometric function). In the interesting 3-pomeron limit ($\beta << 1$) the path integral can be evaluated by the saddle point method with the result

$$F_{T,L}^{D(3),inel}(Q^2, x_P, \beta) = G \; H_{T,L}(1)\frac{e_f^2\alpha^5 N^2\pi}{4}\left(\frac{2a(x_P)}{\pi}\right)^3 x_P^{-1-2\Delta_P}\frac{r_0 Q}{2}$$

$$\beta^{-\Delta_P}\left(\frac{2a(\beta)}{\pi}\right)^{\frac{1}{2}}\exp\left(-\frac{a(\beta)}{2}\ln^2(r_0 Q/2)\right) \tag{16}$$

7

where $G = .915...$ is Catalan's constant, $H_T(1) = 9/2$, $H_L(1) = 1$.

The important features of Eq.(16), pointed out in [13] are

(a) An approximate factorization of the x_P and Q^2 dependences.

(b) Important logarithmic corrections of the form $(\ln(1/x_P))^{-3}$ to the main power law factor $x_P^{-1-2\Delta_P}$. These corrections lower the effective pomeron intercept for diffractive dissociation, in qualitative agreement with the data.

(c) There is a significant scaling violation, because $F_{T,L}^{D(3)}$ depends explicitly on Q^2.

(II) Quasi-elastic component.

It was discussed in [14], where the formulae for diffractive cross-sections in γ^*-dipole collisions were given. From these formulae one can derive the following expression for the diffractive structure functions.

$$
\begin{aligned}
F_T^{D(3),qel}(Q^2, x_P, \beta) &= \frac{Q^4 N_c e_f^2}{2\pi^3 \beta x_P} n_{eff}^2 \int_{r_0}^{\infty} d^2 b \int_0^1 dz \left(z^2 + (1-z)^2 \right) z^2 (1-z^2) \\
&\quad \times \left| \int_0^{r_0} d\rho \, T\left(b, \rho, r_0, \xi \right) K_1\left(\hat{Q}r \right) J_1\left(\hat{M}r \right) \right|^2
\end{aligned}
\tag{17}
$$

and

$$
\begin{aligned}
F_L^{D(3),qel}(Q^2, x_P, \beta) &= \frac{Q^4 N_c e_f^2}{\pi^3 \beta x_P} n_{eff}^2 \int_{r_0}^{\infty} d^2 b \int_0^1 dz \, z^3 (1-z)^3 \\
&\quad \times \left| \int_0^{r_0} d\rho \, T\left(b, \rho, r_0, \xi \right) K_0\left(\hat{Q}r \right) J_0\left(\hat{M}r \right) \right|^2
\end{aligned}
\tag{18}
$$

where
$$
\hat{Q}^2 = z(1-z)Q^2, \quad \hat{M}^2 = z(1-z)M^2 \tag{19}
$$

and $T(b, \rho, r_0, x_P)$ is the amplitude for elastic scattering of a dipole of diameter ρ on a dipole of diameter r_0 at impact parameter b.

In Ref.[14] this amplitude was approximated by its asymptotic form valid for large b which reads

$$
T(b, \rho, r_0, x_P) \approx \pi \alpha^2 \frac{\rho r_0}{b^2} \ln\left(\frac{b^2}{\rho r_0} \right) x_P^{-\Delta_P} \left(\frac{2a(x_P)}{\pi} \right)^{\frac{3}{2}} e^{\frac{a(x_P)}{2}} \ln^2\left(\frac{b^2}{\rho r_0} \right) \tag{20}
$$

8

and for that reason the integration over b was performed from r_0 to ∞ (the meaning of the formula (20) for $b < r_0$ is rather doubtful).

The main qualitative features of this quasi-elastic component, pointed out in [14], are

(a) A similar x_P dependence as the inelastic component, with important logarithmic corrections bringing down the pomeron intercept.

(b) As expected, the quasi-elastic component vanishes at $\beta = 0$ and actually populates significantly only the region $\beta \geq .2$.

(c) The dependence on β of the transversal and longitudinal structure functions is dramatically distinct. F_T dominates in the region $\beta \leq .8$ whereas F_L takes over at small β. The sum of the two components, however, is almost constant in the range $.3 \leq \beta < 1$.

4   Predictions for hard diffraction

The formulae presented in Section 4 were obtained in [13, 14] by calculating first the cross-section of γ^* on a single dipole of a fixed transverse diameter r_0 in the limit of very large impact parameter b. The obtained formulae were then extrapolated until $b_{min} = r_0$ and integrated from b_{min} to ∞. Finally the result was multiplied by n^2_{eff} to account for the number of the dipoles in the target nucleon (determined from the fit of the formula for F_2 to the data).

These approximations allowed to perform explicit calculations and to discuss the general behaviour of diffractive structure functions [13, 14]. They are, however, not valid in the important region where the impact parameter b is of the order of the size of the original dipoles [17] and therefore the results given in the formulae of Section 3 cannot be treated as precise predictions of the QCD dipole picture (ie. of BFKL dynamics) for several reasons.

First, the asymptotic formula for large impact parameter ignores entirely the singularities of the dipole-dipole amplitudes, which become important when the impact parameter is of the order of the size of the colliding dipoles. This defect leads to a serious underestimation in the normalization of the calculated cross-sections[2]. However, the conformal invariance of the BFKL dynamics [21, 22] insures that the general dependence on kinematic variables remains - to a good approximation- unaffected.

---

[2]It was recently shown in [17] that this factor may even well exceed 100.

Second, the cross-section for scattering on a single dipole of the size r_0, even if multiplied by n_{eff}^2, cannot be directly used for the estimation of the cross-section on the nucleon target. The reason is twofold: (i) it is unlikely that all the primary dipoles in the nucleon are of the same size r_0 and thus the distribution of their sizes must be taken into account, (ii) The single-dipole cross-section ignores entirely the distribution of the transverse position of the primary dipoles in the nucleon, i.e. it ignores the effects of the nucleon form-factor. Although these effects are not present in forward scattering amplitudes (and therefore they do not influence the calculation of the total cross-section) they largely determine the momentum transfer dependence and thus reduce significantly the cross-section integrated over momentum transfer to the target nucleon.

To summarize, we note [17] two effects which were not included in the calculations given in [13, 14] and which are expected to affect substantially the normalization of the obtained diffractive structure functions. In this situation before a more precise calculation is available, we treat the normalization of the two components as free parameters, in order to phenomenologically evaluate the main conditions for a test of the unified description of proton structure functions. We thus compare the experimental data to the formula

$$F_2^{D(3)} = N_{inel} F_2^{D(3),inel} + N_{qel} F_2^{D(3),qel} \tag{21}$$

where $F_2^{D(3),inel}$ and $F_2^{D(3),qel}$ are constructed from the formulae (16), (17) and (18) using $F_2 = F_L + F_T$.

Since this procedure can at best be considered only as an exploratory search, we did not try to perform a fit, but simply tried a few values of N_{inel} and N_{qel} to see if one can obtain a qualitative agreement of (21) to the data. In Fig.4 the results of these calculations are shown for $N_{inel} = 16$ and $N_{qel} = 6$. One sees that a general description of the data is quite reasonable for $x_P \leq .01$ except in the region of large β where the Q^2 dependence of the quasi-elastic component is not fully adequate.

We find this result rather satisfactory, given the present status of the theoretical calculations. Thus -although the final answer must wait till more precise QCD dipole calculations are available- our tentative conclusion is that the existing data on rapidity-gap events do not rule out the BFKL dynamics as a correct description of the diffractive phenomena involving virtual photons. Indeed a decisive test will come along with more complete theoretical calculations e.g. [17].

10

5 Conclusions and outlook

In conclusion, we have shown that the BFKL dynamics, as represented by the QCD dipole picture, is is in qualitative agreement with the 3-dimensional data on rapidity-gap events being observed at HERA. Further theoretical work is needed, however, to arrive at more precise conclusions. In particular, it is necessary:

(a) to evaluate the γ^* cross-sections without the large-b approximation used in [13, 14]. The work on inelastic component was recently completed [17] and the quasi-elastic component will be available in the near future.

(b) Since the effects related to the nucleon form-factor are expected to influence significantly the results, a serious phenomenological discussion of the nucleon form-factor in the framework of the QCD dipole picture is required. More precise data on momentum transfer dependence of the diffractive structure functions would be of great help [3].

We feel that this program is feasible and thus one may hope that a unified picture of the high-energy diffractive processes involving the virtual photons, based on BFKL dynamics, may indeed be constructed in the near future.

---

[3]The form-factor effects being unimportant for forward scattering, the measurements of diffraction dissociation at zero momentum transfer would of course bring an important information to the problem we consider. At this point one may notice that also the measurements of the virtual photon shadowing in nuclei (which depends mainly on forward diffractive amplitudes [23]) could provide another practical method to learn about the diffraction at zero momentum transfer.

References

[1] H1 coll., *Nucl.Phys.* **B470** (1996) 3

[2] H1 coll., *"Inclusive measurement of Diffractive Deep-Inelastic ep Scattering"*, DESY 97-158, August 1997.

[3] For a recent review, see J.Bluemlein, J.Huston, C.Royon, R.Yoshida, *Summary of Working group I: hadron structure*, P.Newman, *Colour singlet exchange in ep interactions*, D.Soper, *Diffraction in DIS and elsewhere*, Summary talks given at the "DIS 97" conference, Chicago.

[4] G. Altarelli and G. Parisi, *Nucl. Phys.* **B126** (1977) 298; V.N. Gribov and L.N. Lipatov, *Sov. Journ. Nucl. Phys.* **15** (1972) 438 and 675. Yu.L. Dokshitzer, *Sov. Phys. JETP* **46** (1977) 641.

[5] M.Glück, E.Reya, A.Vogt, *Z.Phys.* **C53** (1992) 127, *Phys.Lett.* **B306** (1993) 391.

[6] V.S.Fadin, E.A.Kuraev, L.N.Lipatov, *Phys. Lett.* **B60** (1975) 50; I.I.Balitsky and L.N.Lipatov, *Sov.J.Nucl.Phys.* **28** (1978) 822.

[7] G.Ingelman, P.Schlein, *Phys.Lett.* **B152** (1985) 256.

[8] M.L.Good and W.D.Walker, *Phys. Rev.* **120** (1960) 1857. H.I.Miettinen and J.Pumplin, *Phys.Rev.* **D18** (1978) 1696.

[9] A.Edin, G.Ingelman, J.Rathsman, *Phys.Lett.* **B366** (1996) 371, *Z.Phys.* **C75** (1997) 57, W.Buchmüller, A.Hebecker, *Phys.Lett.* **B355** (1995) 573, *Nucl.Phys.* **B476** (1996) 203

[10] A.H.Mueller, *Nucl. Phys.* **B415** (1994) 373; A.H.Mueller and B.Patel, *Nucl. Phys.* **B425** (1994) 471; A.H.Mueller, *Nucl. Phys.* **B437** (1995) 107.

[11] See also, N.N.Nikolaev and B.G.Zakharov, *Zeit. für. Phys.* **C49** (1991) 607.

[12] H.Navelet, R.Peschanski, Ch.Royon, *Phys.Lett.* **B366**, (1996) 329; H.Navelet, R.Peschanski, Ch.Royon, and S.Wallon, *Phys.Lett.* **B385** (1996) 357.

[13] A.Bialas, R.Peschanski, *Phys. Lett.* **B378** (1996) 302; A.Bialas, *Acta Phys.Pol.* **B27** (1996) no. 6.

[14] A.Bialas, R.Peschanski, *Phys.Lett.* **B387** (1996) 405.

[15] M.Genovese, N.N. Nikolaev and B.G.Zakharov *Sov. Phys. JETP* **81** (1995) 625,633.

[16] A.Bialas, *Acta Phys.Pol.* **B28** (1997) 1239.

[17] A.Bialas, H.Navelet, R.Peschanski, Saclay preprint T97/131, hep-ph/9711236.

[18] J.Bjorken, J.Kogut, D.Soper, *Phys.Rev.* **D3** (1971) 1382.

[19] G. Camici, M.Ciafaloni, hep-ph/9707390.

[20] H1 Coll., *Phys.Lett.* **B393** (1997) 452.

[21] L.N. Lipatov *Zh. Eksp. Teor. Fiz.***90** (1986) 1536 (Eng. trans. *Sov. Phys. JETP* **63** (1986) 904).

[22] H.Navelet, R.Peschanski, preprint SACLAY-SPHT-96-136, to be published in *Nucl. Phys.*; H.Navelet, S.Wallon, preprint SACLAY-SPHT-97-023 to be published in *Nucl. Phys.*

[23] A.Bialas, W.Czyz and W. Florkowski, Phys. Rev. **D55** (1997) 6830; A.Bialas and W.Czyz, submitted to Acta Physica Polonica B.

FIGURE CAPTIONS

Figure 1 Fig.1a. Inelastic diffraction (component I)
Fig.1b. Quasi-elastic diffraction (component II)

Figure 2 Comparison of the 4-parameter fit with the H1 data. The validity of the prediction extends beyond the domain included in the fit. We note a discrepancy at high x, high Q^2 due, in particular, to the absence of the valence contribution not considered in the present model.

Figure 3 Comparison of our prediction for the longitudinal structure function F_L and the H1 data. The prediction is somewhat lower than the measurement, but more precise data are needed to make more precise tests.

Figure 4 Prediction for the total (longitudinal + transverse) diffractive structure function, see text. Dotted lines: the inelastic component I; Dashed lines the quasi elastic component II; Full line: the sum of both components (Note that at $\beta \approx 1$, the inelastic component is almost 0 and the dashed line coincides with the full line and thus is not apparent on the plot).
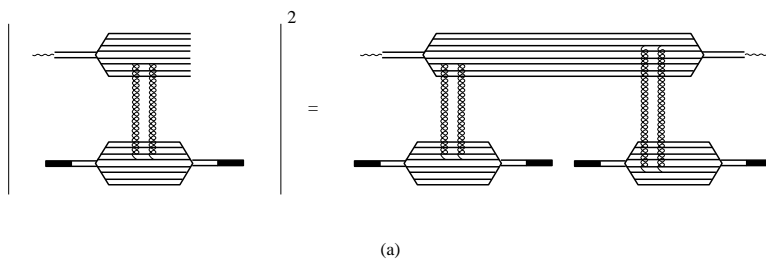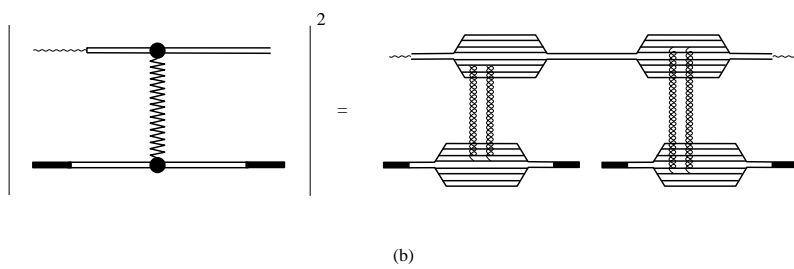
(a)

Figure 1

15

(b)

Figure 1

Q²=1.5 beta=0.01	Q²=4.5 beta=0.01	Q²=7.5 beta=0.01	Q²=9 beta=0.01	Q²=12 beta=0.01	Q²=18 beta=0.01	Q²=28 beta=0.01	Q²=35 beta=0.01	Q²=75 beta=0.01
Q²=1.5 beta=0.04	Q²=4.5 beta=0.04	Q²=7.5 beta=0.04	Q²=9 beta=0.04	Q²=12 beta=0.04	Q²=18 beta=0.04	Q²=28 beta=0.04	Q²=45 beta=0.04	Q²=75 beta=0.04
Q²=1.5 beta=0.1	Q²=4.5 beta=0.1	Q²=7.5 beta=0.1	Q²=9 beta=0.1	Q²=12 beta=0.1	Q²=18 beta=0.1	Q²=28 beta=0.1	Q²=45 beta=0.1	Q²=75 beta=0.1
Q²=1.5 beta=0.2	Q²=4.5 beta=0.2	Q²=7.5 beta=0.2	Q²=9 beta=0.2	Q²=12 beta=0.2	Q²=18 beta=0.2	Q²=28 beta=0.2	Q²=45 beta=0.2	Q²=75 beta=0.2
Q²=1.5 beta=0.4	Q²=4.5 beta=0.4	Q²=7.5 beta=0.4	Q²=9 beta=0.4	Q²=12 beta=0.4	Q²=18 beta=0.4	Q²=28 beta=0.4	Q²=45 beta=0.4	Q²=75 beta=0.4
Q²=1.5 beta=0.65	Q²=4.5 beta=0.65	Q²=7.5 beta=0.65	Q²=9 beta=0.65	Q²=12 beta=0.65	Q²=18 beta=0.65	Q²=28 beta=0.65	Q²=45 beta=0.65	Q²=75 beta=0.65
Q²=1.5 beta=0.9	Q²=4.5 beta=0.9	Q²=7.5 beta=0.9	Q²=9 beta=0.9	Q²=12 beta=0.9	Q²=18 beta=0.9	Q²=28 beta=0.9	Q²=45 beta=0.9	Q²=75 beta=0.9